Pol. J. Environ. Stud. Vol. 33, No. 2 (2024), 1899-1914
DOI: *10.15244/pjoes/173108* ONLINE PUBLICATION DATE: 2023-12-28

Original Research

Simulation and Analysis of Land Use Change in Jianghuai Hilly Area Based on PLUS Model

Liuyang Xu, Weiling Guo*, JiAng Jia

School of Geomatics, Anhui University of Science & Technology, NO. 168 Taifeng Road, Huainan 232001, China

Received: 26 June 2023
Accepted: 1 October 2023

Abstract

The Jianghuai-Huai Hilly Region (JHHR), being a crucial agricultural and forestry hub within the Yangtze River Economic Belt, holds immense significance in investigating land use dynamics under diverse scenarios. Such exploration not only facilitates the sustainable utilization of land resources but also contributes to ecological environmental preservation and the advancement of regional economic and social development. This study aims to analyze the spatial and temporal characteristics and driving forces of land use in JHHR over the past three decades (1990-2020) using 18 driving factors selected from both the natural environment and social economy. We have considered four different scenarios, including Natural Development (ND), Rapid Development (RD), Cultivated Land Protection (CLP), and Ecological Protection (EP). We used the PLUS model to simulate land use changes in JHHR until 2040, and we analyzed the spatial distribution pattern of land under different objectives. The results show that: (1) The main types of land use in the Jianghuai hilly area are arable land and woodland. In the past 30 years, the land use changes have been relatively stable, the area of arable land and woodland has continued to decrease, and the construction land has continued to grow; unused land and grassland have the highest dynamic degree, with the highest comprehensive dynamic degree from 2000 to 2005, at 0.42%; (2) In 2020, the simulation accuracy of land use in different time spans is high, with a Kappa coefficient higher than 0.85 and an overall accuracy higher than 92%, both higher than the standard. (3) The main driving factors for land expansion from 1990 to 2020 were natural factors such as DEM and slope, and the driving forces for construction land mainly came from socio-economic factors. (4) There are obvious gaps in land use changes under different scenarios. A comprehensive comparison of the growth of other types of land use to varying degrees under the ecological protection scenario and under the protection of ecological land use can be used as the optimal development scenario model. The scenario simulation can provide an effective reference for the rational planning and management of land in the Jianghuai hilly area.

Keywords: PLUS model, land use change, multi-scenario simulation, Jianghuai hilly area

*e-mail: wlguo28@aust.edu.cn

Introduction

Land is the foundation of human civilization and provides a habitat for various ecosystems. However, the development of human society has continuously impacted the functions and structures of land [1], such as modern urbanization, agricultural production methods, and industrialization efforts [2]. Land use change, which refers to changes in land use types and their proportions within a given spatial unit [3, 4], can reflect dynamic changes in land cover influenced by natural environmental, economic, and social factors [5]. Current research on land use change is focused on identifying spatial differentiation characteristics, and intrinsic driving forces, evaluating sustainability, and simulating future changes [6-8], These simulation models can help people understand the interconnection between land, economy, society, and the environment, and promote sustainable development and resource use [9], Therefore, it is important for policymakers and planners to better manage and plan for present land.

As computing power and data availability continue to advance, land use simulation models have evolved from empirical rules and statistical models to the current neural networks [10]. Among the models used for land use change research, prominent ones include CA-Markov [11], SD [12], FLUS [13], and others. These models effectively predict land use changes by considering a variety of factors, making them widely used in the field [14, 15]. However, these models have limitations in simulating land use changes at the patch scale and explaining the complex drivers behind these changes [16, 17]. The PLUS model is introduced to address these issues and achieve higher accuracy. The PLUS model is a rule mining framework that combines land expansion analysis (LEAS) and a CA model based on a multi-type stochastic seed mechanism [18, 19]. The PLUS model has garnered substantial attention from researchers, leading to numerous significant findings. For instance, Shihe Zhang et al. [20] utilized the PLUS model to investigate the landscape pattern of the Fujian delta region in 2050 and analyze the ecological risk associated with land change under different scenarios; Similarly, Tongli Niu et al. [21] employed the PLUS model to simulate and analyze land use changes in the Yangtze River basin in 2050, comparing three scenarios: inertia development, CLP, and ecological priority. The study verified the model's strong simulation capabilities in capturing land use changes in the Yangtze River basin.; Another notable study by Li Jun et al. [22] combined the PLUS model with the InVEST model to predict land use changes and carbon stock variations under different scenarios in Kunming City. By analyzing the impact of different land use changes on carbon stock, the research shed light on the broader implications of land use decisions. Given its higher simulation accuracy and adaptability, the PLUS model stands out as this study's chosen land use prediction model. Its advanced features and effectiveness in capturing complex land use dynamics make it an ideal tool for exploring and understanding future land use patterns.

This study aims to investigate the spatial and temporal changes in land use, and its drivers under different scenarios. The ultimate goal is to provide valuable insights for decision-makers in hilly areas by informing land management policies and planning. Using the PLUS model, we investigate the spatial and temporal characteristics of land use distribution from 1990 to 2020. We also predict the spatial pattern of land use in JHHR under various scenarios for 2040 using cost matrix and domain factor settings. By exploring the spatial and temporal characteristics of land use in the JHHR, and providing analyses of future scenarios, this research bridges the gap between theoretical understanding and practical decision-making. The study contributes to the body of knowledge that supports effective land management policies and planning, ensuring sustainable development in hilly areas and promoting a harmonious coexistence between human activities and the environment.

Study Area and Data Sources

Overview of the Study Area

The Jianghuai Hilly Area is located at 115°49′E-119°35′ and 30°12′-34°17′N (Fig. 1), surrounded by the Yangtze River and the Huai River, mainly containing Chuzhou City, Hefei City, Liuan City, and Maanshan City, with a total area of 44,416.23 km^2 and a total population of 12,096,600. The terrain is mainly hilly and mountainous, decreasing from the south to the northeast, with an average elevation of 150 m. The landscape is dominated by hills and mountains, including the southern foot of Dabie Mountain, hilly beaches and basin mountains, with undulating terrain, mountain peaks and crags, and intertwined rivers and lakes. The climate is a subtropical monsoon climate with rainy summer, high temperatures, the annual average temperature around 15ºC, and annual precipitation between 800~1600 mm. JHHR is one of the important economic regions in the Anhui Province of China, and the economy continues to maintain a fast development momentum, and also has rich natural and cultural resources, especially the agricultural resources and red cultural resources in the Huaihe River Basin, etc.

Data Source and Pre-Processing

The research data for this study encompass three main types: land use data, socio-economic data, and natural environment data. Detailed information on these data sources is presented in Table 1. To obtain the land use data, we accessed the Institute of Remote Sensing Information Processing at Wuhan University. Specifically, the JHHR land use data were reclassified

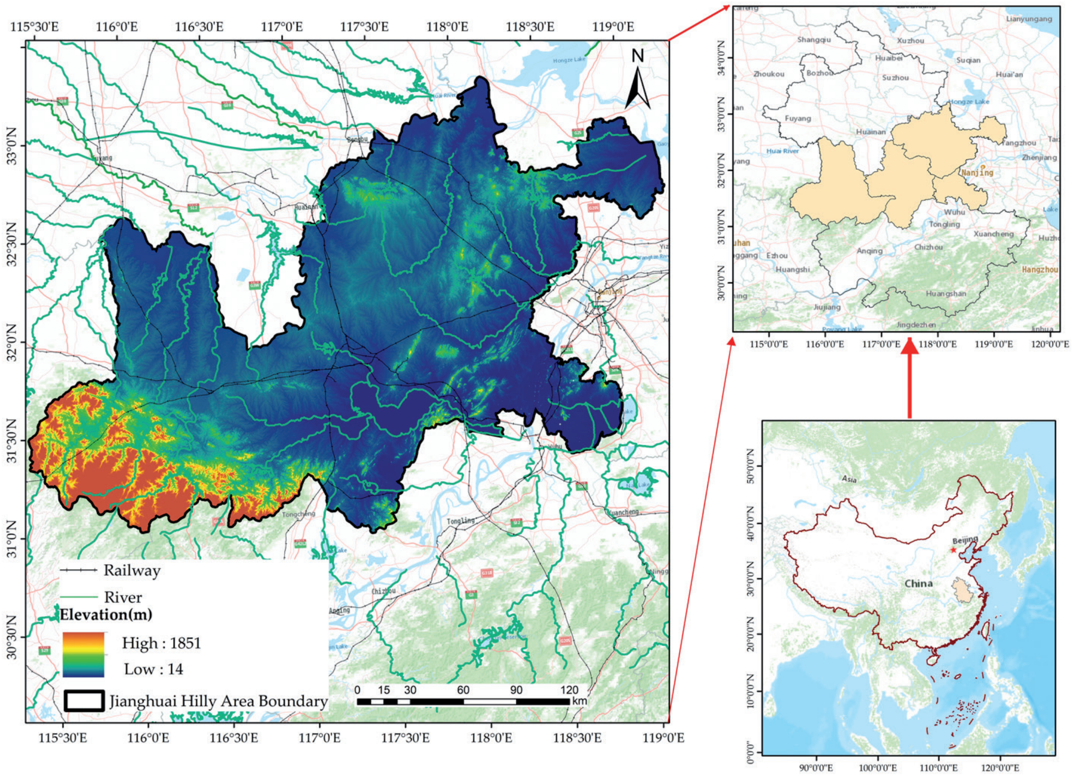

Fig. 1. Study area.

into six categories, namely cultivated land, forest land, grassland, water area, construction land, and unused land, utilizing the Chinese land use classification standard as a reference. The road network data, which is essential for analyzing transport patterns and their influence on land use, was obtained from OpenStreetMap. Extraction techniques were used to extract and utilized the road data for analysis. The DEM (Digital Elevation Model) data used in the study were obtained from ASTGTM GDEM. Additionally, we calculated slope data based on the DEM data, providing valuable insights into the topography of the study area. Various environmental variables, including rainfall, temperature, soil properties, and night light remote sensing data, were acquired from the Resource and Environment Data Center of the Chinese Academy of Sciences. These data sources played a crucial role in understanding and assessing the natural environmental factors influencing land use patterns. All the collected data were processed using ArcGIS software. To ensure consistency and compatibility, the data were resampled to a common resolution of 30 m x 30 m and projected using UTM coordinates in the WGS1984 coordinate system. By utilizing these diverse data sources and employing rigorous processing techniques, the study can offer comprehensive and reliable insights into the complex interplay between land use dynamics, socio-economic factors, and the natural environment in the research area.

Research Methodology

Land Use Dynamic Attitude and Transfer Matrix

Single dynamics refers to the degree of change of a certain type of land use within a certain period of time, that is, the degree of movement of a certain use to other uses; comprehensive dynamics refers to the comprehensive changes of multiple types of land use [23, 24]. The calculation formula is as follows:

$$K = \frac{U_b - U_a}{U_a} \times \frac{1}{T} \times 100\% \tag{1}$$

$$LC = \frac{\sum_{i=1}^{n} \Delta LU_{a-b}}{2LU} \frac{1}{T} \times 100\% \tag{2}$$

Where: K denotes the kinetic attitude of a particular land class during the study area; LC denotes the combined kinetic attitude of land classes in the study area; U_a and U_b refer to the area at the beginning and end of the land class, respectively; T denotes the study period; ΔLU_{a-b} is the absolute value of the data for the transition from land class a to land class b in time T.

The land use transfer matrix is a matrix of the inter-transformation relationships and quantities between different land use types at a certain time [25, 26]. It can provide an in-depth analysis of the evolution and trend of land spatial patterns by reflecting the change process between different land use types [27]. The expressions are as follows:

Table 1. Data source information.

Data Type	Data Name	Time	Data source
Land Use Data	Land Use Data	1990-2020	Institute of Remote Sensing Information Processing, Wuhan University (http://irsip.whu.edu.cn/)
Natural Factors	Average annual rainfall /mm	1990-2020	Data Center for Resources and Environment, Chinese Academy of Sciences (https://www.resdc.cn/)
	Average annual temperature /ºC		
	Soil type	/	
	DEM/m	/	ASTGTM GDEM (http://gdem.ersdac.jspacesystems.or.jp)
	Slope	/	ArcGIS calculates the DEM to obtain
	Distance from river/m	2023	OpenStreetMap (https://www.openstreetmap.org/)
Socio-economic factors	Distance to primary road/m	2023	OpenStreetMap (https://www.openstreetmap.org/) ArcGIS Euclidean distance
	Distance from secondary road/m		
	Distance to tertiary road/m		
	Distance to highway/m		
	Distance to railway/m		
	Distance to school/m		
	Distance to city/m		
	Distance to township/m		
	Distance from countryside/m		
	Nighttime Lighting Index	1990-2020	Data Center for Resources and Environment, Chinese Academy of Sciences(https://www.resdc.cn/)
	Population density (person/km^2)		
	GDP		

$$P = \begin{bmatrix} A_{11} & A_{12} & \cdots & A_{1n} \\ A_{21} & A_{22} & \cdots & A_{2n} \\ \vdots & \vdots & A_{ab} & \vdots \\ A_{n1} & A_{n2} & \cdots & A_{nn} \end{bmatrix} \tag{3}$$

Where: A represents the area of the land class; i, j (i, j = 1, 2, 3···n) denote the early and late ground classes of the study, respectively; n is the number of land classes.

PLUS Model

PLUS model is a patch generation land use simulation model based on multi-type stochastic patch seeds, an improved CA model based on FLUS model, which integrates land expansion analysis strategy (LEAS) and multi-type stochastic seeds (CARS) [18], addressing the potential drivers of land use change process and spatial-temporal dynamic multi-type land use that are lacking in CA model generation and land patches [28, 29]. The model obtains the development probability of each factor on land expansion by LEAS module, predicts the amount of future land use by MarKov model [30], and performs the patch evolution of land use types by CARS under the constraints of total probability, adaptive coefficient, domain effect, and transfer matrix [20, 31] to obtain the simulated distribution map of future land use.

Land Expansion Analysis Strategy (LEAS)

LEAS simplifies the calculation of land class change for multiple classes of feature change by transforming the conversion rule mining for each land class into obtaining the probability of change and probability of inertia for each land use type, and then exploring the expansion and drivers of each land class for mining by the Random Forest Classification (RFC) algorithm [10] to obtain the development probability of each land class and the weight of drivers on the land class.

In this paper, we utilize random sampling and random forest algorithm under LEAS module to obtain the growth probability of each land use type based on land use data from 1990-2020, combining 18 drivers [32] with the following equation:

$$P_{i,t}^{x}(v) = \frac{\sum_{n=1}^{L} N(h_n(v) = x)}{L} \tag{4}$$

where: $P_{i,t}^{x}(v)$ is the probability of growth of land use type t at spatial unit i; v is a vector composed of driving factors; N(.) is the indicator function of the decision tree;

Table 2. Domain weights by land use type.

Year	Cropland	Woodland	Grassland	Water	Construction Land	Unused land
1990-2000	0.1	0.4647	0.1	0.4535	1	0.1
2000-2010	1	0.4245	0.1	0.1654	0.1	0.4112
2000-2005	1	0.5820	0.1	0.2478	0.1	0.1908
2005-2010	1	0.1676	0.1	0.1	0.1	0.8139
2015-2020	0.4656	1	0.1	0.4002	0.1	0.9546

h_n(v) is the predicted land use type of the nth decision tree of vector v; L is the number of decision trees; when x = 1, it means that other land use types are transformed to t, and when x = 0, there is no transformation to land type t.

CA Model Based on Multi-Class Random Patch Seeding (CARS)

The CARS module is a patch generation mechanism based on multiple types of stochastic seeds for land use, and simulates land use dynamics based on the development probability, domain extent, adaptive inertia, domain weights, and transfer matrix of each type of land use [33-35], where domain extent, diffusion coefficient, and decreasing threshold are the defaults.

(1) Domain weights indicate the intensity of land type conversion to other land types [36] and are calculated in this paper based on previous land use data with the following equation:

$$X_i = \frac{TA_i - TA_{min}}{TA_{max} - TA_{min}} \tag{5}$$

Where: X_i is the domain weight parameter of the i-th land type, range 0~1; TA_i is the area of land use type change in the study interval; TA_{max}, TA_{min} denote the maximum and minimum values of land use type change in the study interval, respectively. The calculated weights are shown in Table 2.

(2) The overall probability of each type of land use was calculated using a stochastic patch generation mechanism to simulate the change of each land use under the setting of each land use growth probability constraint [37] with the following equation:

$$NP_{i,k}^{d=1,t} = P_{i,k}^{d=1} \times \Omega_{i,k}^{t} \times D_k^t \tag{6}$$

where: $NP_{i,k}^{d=1,t}$ denotes the integrated probability; $P_{i,k}^{d=1}$ is the probability of suitability of land class k for spatial unit i: D_k^t is this is an adaptive driving coefficient that reflects the degree of future land use demand for land use type k. This coefficient depends on the difference between the amount of land use at the current iteration t and the target demand for land use type k; $\Omega^t_{i,k}$ is the domain effect of spatial cell i, i.e., the proportion of land use components covered by k in the next neighborhood.

Scenario Setting

In order to investigate the land use changes of JHHR under different scenarios, based on the NP scenario, cultivated land conservation scenario, the ecological conservation scenario and the RD scenario, and with reference to the existing research results [38-40], each cost matrix is set up in Table 3 below:

Table 3. Land use transfer matrix for the four scenarios.

	NP scenarios						CLP scenarios						EP scenarios						RD Scenario					
	a	b	c	d	e	f	a	b	c	d	e	f	a	b	c	d	e	f	a	b	c	d	e	f
a	1	1	1	1	1	1	1	0	0	0	0	0	1	1	1	1	1	1	1	0	0	0	1	0
b	1	1	1	1	1	1	1	1	1	0	1	1	0	1	0	0	0	0	1	1	0	0	1	0
c	1	1	1	1	1	1	1	1	1	1	1	1	0	1	1	1	0	0	1	1	1	1	1	0
d	1	1	1	1	1	1	1	0	1	1	1	1	0	0	0	1	0	0	1	1	0	1	1	0
e	1	1	1	1	1	1	0	0	0	0	1	0	0	0	0	0	1	0	0	0	0	0	1	0
f	1	1	1	1	1	1	1	1	1	1	1	1	1	1	1	1	1	1	1	1	1	1	1	1

Note: NP-Natural Development; RD- Rapid Development; CLP- Cultivated land protection; EP- Ecological Protection

Results and Analysis

Spatial and Temporal Land Use Change Characteristics

Analysis of the Current Situation of Land Use Types

The land classification map of the JHHR from 1990 to 2020 (Fig. 2) and the proportion of each type of land use (Fig. 3) reveal that JHHR is primarily dominated by cultivated land and forest land, which for many years have accounted for more than 85% of the total area. The remaining area is shared by water and construction land, while grassland and unused land make up the smallest proportion. Regarding spatial distribution, the first part to the north of the southern boundary of JHHR is mainly dominated by forest land. The second part is characterized by construction land and watershed, mostly found in the middle and on the edge of the region, with the provincial capital city's construction land aspect dominating and concentrating in this area. Lakes are mainly found in and around Chaohu Lake. Meanwhile, the third part is dominated by cultivated land, which is mainly distributed in the middle and upper part of the hilly area. Specifically, forest land is mainly distributed in the hilly and mountainous areas of the Dabie Mountain Ecological and Economic Zone, while cultivated land is mostly distributed in the plain area. Given the changing land use in this region, it is important to pay attention to the significant impact of rational planning and management of land resources on protecting and enhancing the quality of the ecological environment.

Land Use Dynamic Attitude and Transfer Matrix Analysis

According to the data provided in Table 4, it is evident that the comprehensive dynamic attitude towards land use in JHH remained stable from 1990 to 2020. The highest rate was observed during the period of 2000-2005, reaching 0.42%, while it maintained around 0.2% during other periods. Analyzing the dynamic attitude towards individual land use types, it can be observed that the largest trend was observed in unused land and grassland, whereas cropland and forest land exhibited the smallest changes. The order of magnitude, from highest to lowest, was construction land, unused land, grassland, water area, cropland, and forest land. Throughout six periods reflecting the dynamics of land use, there was a consistent decline in grassland coverage, accompanied by a notable increase in construction land. Other land use types experienced fluctuating changes of decrease-increase-decrease. These comprehensive changes indicate that over 30 years, JHHR has undergone significant expansion in construction land, leading to occupation and reduction of other land use categories. As a result, the overall economic benefits have become predominant.

The data presented in Table 5 reveal significant changes in land use patterns from 1990 to 2020. There has been a noticeable decline in the area of cultivated land, forest land, grassland, water area, and unused land, while the area occupied by construction land has experienced an increase. Particularly striking is the transferred area of construction land, which reached a substantial 2,280.03 square kilometers, accounting for 44.96% of the total transferred area. The primary source of these transferred areas is cultivated land, followed by forest land, constituting 31.38% and 13.80% respectively. Additionally, the transferred land primarily originates from cultivated land, forest land, and water area, with transferred areas of 3,273.36 square kilometers, 905.86 square kilometers, and 773.91 square kilometers, amounting to 64.55%, 17.86%, and 15.26% respectively. The expansion of construction land has consequently led to a decline in cultivated land and forest land. Fig. 4 further demonstrates the obvious transformation of various land types, with continuous outward transfers of cultivated land and gradual expansion of the

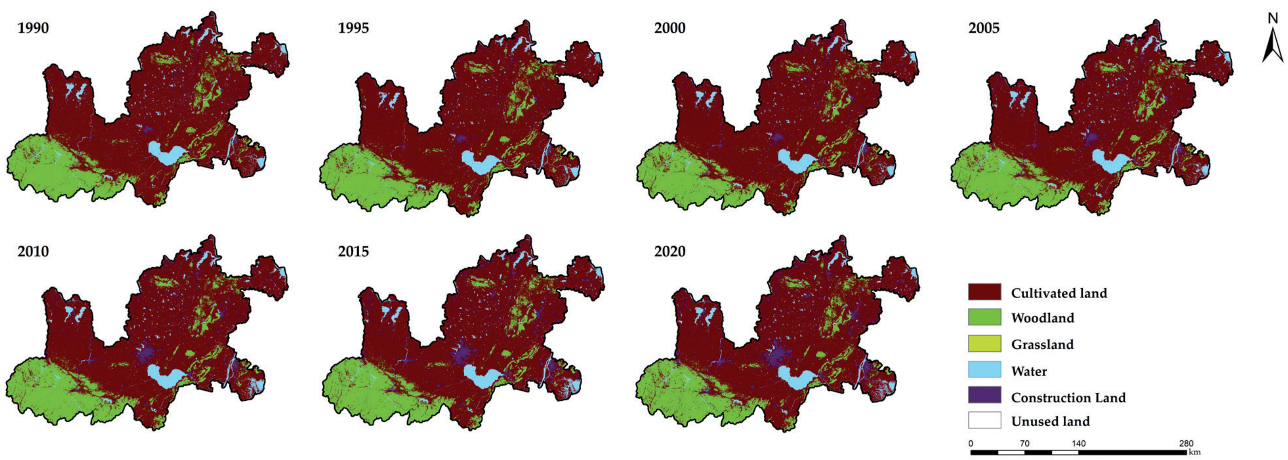

Fig. 2. 1990-2020 Land Use Classification Map.

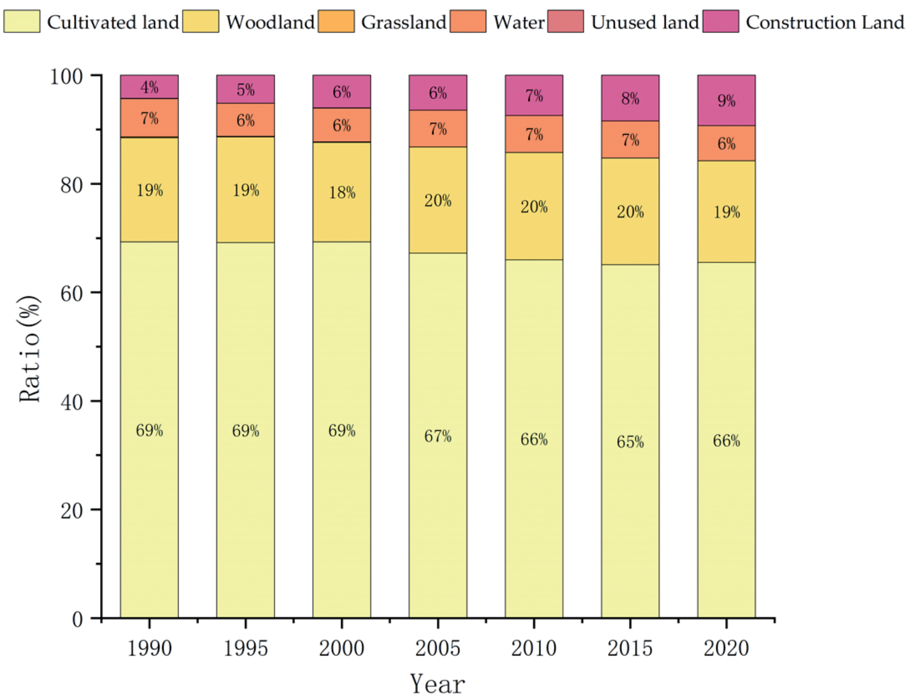

Fig. 3. Percentage of land use by category from 1990 to 2020.

Table 4. Land use dynamic attitude 1990-2020.

Year / Feature Type		1990-1995	1995-2000	2000-2005	2005-2010	2010-2015	2015-2020	1990-2020
Single land use dynamic attitude	1	-0.04	0.03	-0.60	-0.37	-0.27	0.13	-1.09
	2	0.29	-1.14	1.31	0.21	-0.14	-0.92	-0.48
	3	-8.29	-8.25	-3.02	-1.67	-2.33	-12.22	-18.16
	4	-2.75	0.51	1.61	0.15	0.00	-1.06	-1.77
	5	5.03	-6.90	-8.94	-14.61	-13.10	14.24	-18.56
	6	4.13	3.44	1.27	3.06	2.76	2.05	23.51
Integrated land use dynamic attitude		0.23	0.23	0.42	0.25	0.2	0.26	1.00

Note: 1- Cultivated land; 2- Woodland; 3- Grassland; 4- Water; 5- Unused land; 6- Construction area.

construction land area. These transformations mirror those observed in other periods, except for the period spanning from 2000 to 2010.

PLUS Model Accuracy Check

Overall Accuracy of PLUS Model

Based on the actual land use data in 2010, we utilized the FLUS model and PLUS model in conjunction with natural economic factors and other variables to develop an analysis strategy for land expansion in the Jianghuai-Huai Hilly Region (JHH). Consequently, we predicted the land use for 2020 and constructed a confusion matrix to compare the actual land use data with the simulated prediction data. We calculated the overall accuracy and Kappa coefficient for different land use types and presented the results in Table 6 (Area Validation) and Fig. 5 (Spatial Distribution Comparison). The simulation results for 2020 using the FLUS model yielded a Kappa coefficient of 0.79, with an overall accuracy of 87.36%. On the other hand, the PLUS model achieved a higher Kappa coefficient of 0.85 and an overall accuracy of 92.06%. The comparison shows that the PLUS model outperformed the FLUS model in terms of accuracy. However, it is important to note that the different ways of calculating these values influence the synthesis of results. Furthermore, the PLUS model exhibited larger relative errors for grassland and unutilized land, at 16.85% and 17.37% respectively. This can be attributed to the small size and scattered distribution of these land types, making them susceptible to encroachment by

Table 5. Land Use Transfer Matrix 1990-2020.

Land Use Type		2020						Total	Total Transfers Out
		1	2	3	4	5	6		
1990	1	27513.55	676.65	1.61	442.76	0.20	2152.11	30786.91	3273.35
	2	859.27	7616.40	1.621	4.26	0.04	40.65	8522.26	905.85
	3	22.39	14.35	1.99	7.79	0.08	10.628	57.24	55.25
	4	691.59	8.72	0.01	2372.96	0.21	73.36	3146.87	773.91
	5	0.54	0	0.02	4.64	0.03	3.28	8.52	8.49
	6	17.27	0.09	0.002	36.09	0.02	1840.91	1894.41	53.49
Total		29104.63	8316.23	5.26	2868.52	0.61	4120.95	44416.23	/
Transfer to total		1591.08	699.82	3.26	495.56	0.58	2280.03	/	/

Note: 1- Cultivated land; 2- Woodland; 3- Grassland; 4- Water; 5- Unused land; 6- Construction area.

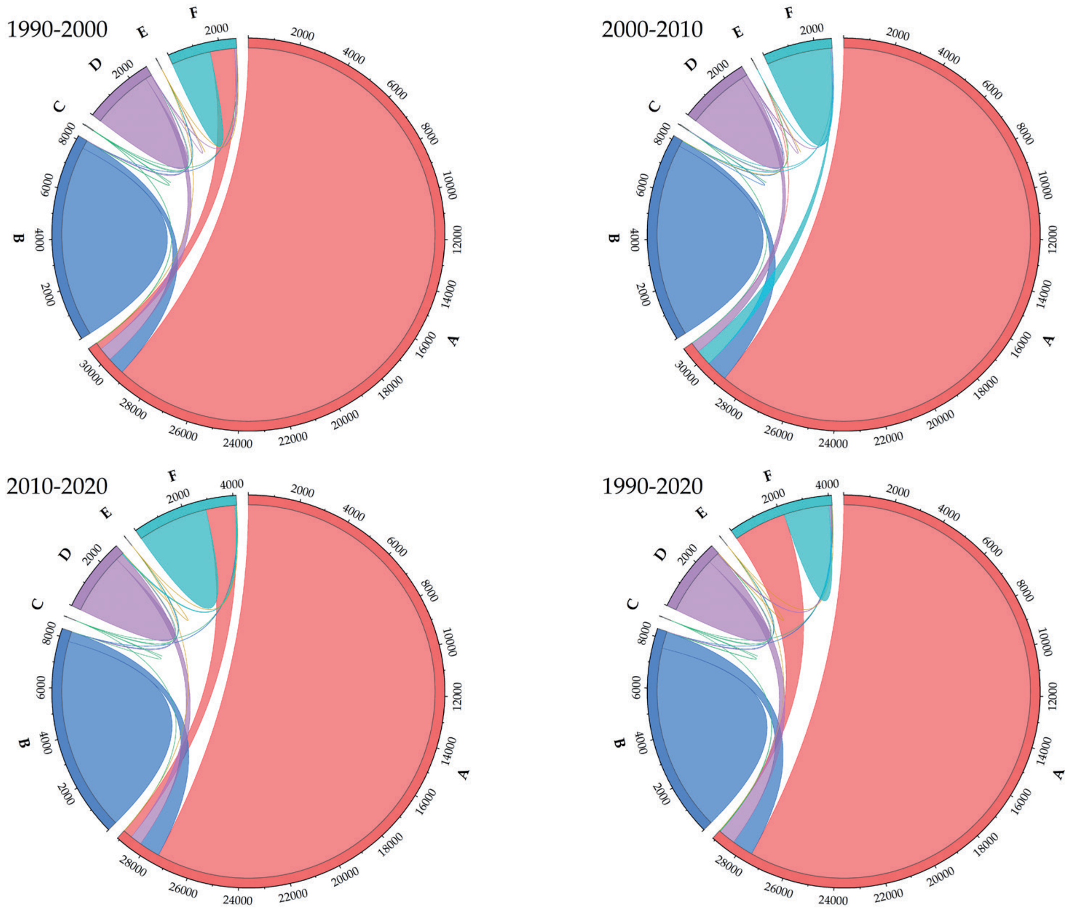

Fig. 4. Map of each land use transfer matrix for the years 1990-2020 JHHR. The outer arcs divided by nodes in the chord diagram reflect the amount of transfer between different types of land areas, the sectors moving clockwise represent the amount of transfer out, the sectors moving counterclockwise represent the amount of transfer in, and the width of the connecting lines represent the size of the transfer.

other features during the simulation. Nonetheless, the overall accuracy met the requirements, demonstrating that the PLUS model effectively meets the desired objectives.

Simulation accuracy under different time spans

To assess the accuracy of the model over different time periods, an investigation was conducted on the simulated land use data for 2000 and 2010, projected to 2010 and 2015 with time spans of 10 and 5 years, respectively. These simulated data were then used as a basis for predicting land use in 2020 using the same approach. The simulation accuracy was then compared, as depicted in Fig. 6. The Kappa coefficients and overall accuracy of the simulations for the year 2020, considering time spans of 5 and 10 years, were found to be 0.86 (92.65%) and 0.85 (92.01%), respectively. These results highlight a relatively minor difference in simulation accuracy between the two-time spans. Notably, the primary discrepancies were observed in the transition zones between forest land, cropland, and areas designated for construction. These findings underscore the model's consistent performance in predicting land use dynamics over various time intervals. Despite slight variations, the overall accuracy remained highly, providing valuable insights into the evolving landscape and aiding in informed decision-making.

Table 6. Validation of land use area projections for 2020.

Land Use Type	Cropland	Woodland	Grassland	Water	Unused land	Construction Land
Actual Area	29104.63	8316.23	5.26	2868.52	0.61	4120.95
Simulated Area	26684.42	8028.80	4.37	2589.18	0.51	4282.10
Relative Error	8.31	3.45	16.85	9.73	17.37	-3.91

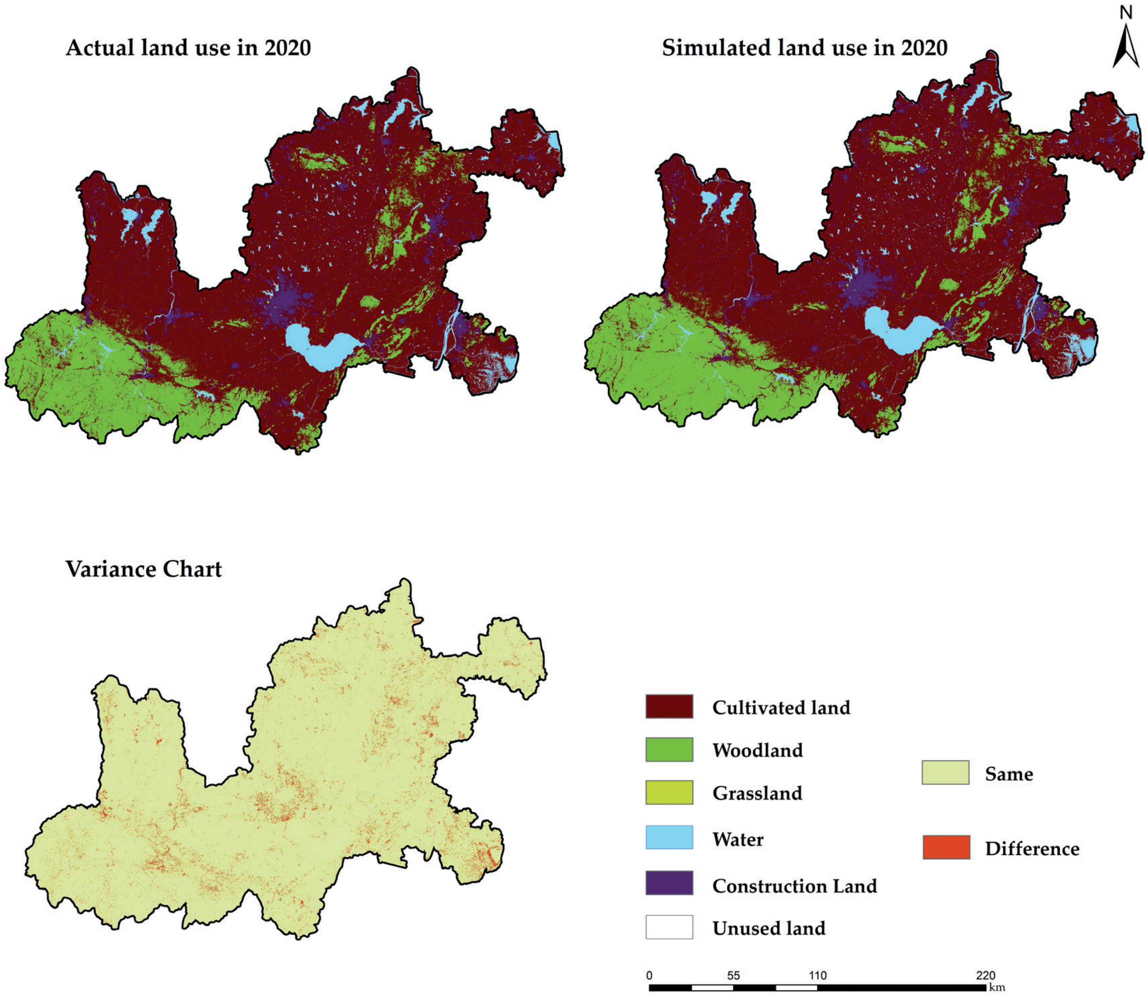

Fig. 5. Map of actual land use and simulated differences in 2020.

Analysis of Driving Forces of Land Use Change in Jianghuai Hilly Area

Land use changes arise from a complex interplay of factors, including population growth, urbanization, and policy demands. These factors often lead to shifts and alterations in the way land is utilized. In the present study, we have examined a comprehensive set of 18 natural and socio-economic factors to investigate their respective contributions to land expansion and the probability of expansion at individual sites. The LEAS module was employed for this analysis, and the findings are presented visually in Fig. 7. Among the different land types, cultivated land and grassland exhibit a strong dependence on natural factors such as Digital Elevation Model (DEM), slope, and temperature. Additionally, the distribution of vegetation is influenced by the unique geographical characteristics of each area. Woodland, on the other hand, is significantly influenced by factors such as population density and DEM. Human activities and demand for natural resources play a crucial role in driving changes in woodland cover. The expansion of watersheds is strongly influenced by rainfall patterns and DEM. Varied rainfall intensities and topographic attributes contribute significantly to the aggregation of watersheds, shaping their spatial extent. The expansion of unused land is primarily driven by DEM and slope, as topographic conditions serve as constraints leading to alterations in land use patterns across different regions. In the case of construction land, socio-economic factors take precedence. The intricate relationship between transportation infrastructure, economic factors, and the planning of urban expansion determines the course of change in the urban landscape. These socio-economic variables are fundamental drivers influencing the dynamics of urban expansion, as presented in Fig. 8.

Land Use Simulation under Multiple Scenarios

Based on the 2020 land use data, land use simulations were conducted under four different scenarios based on the calculated land use expansion probabilities and transfer matrices to predict the spatial distribution pattern of land use in JHHR in 2040, The simulation results and the current status of land use under different scenarios are shown in Fig. 9 and Table 7.

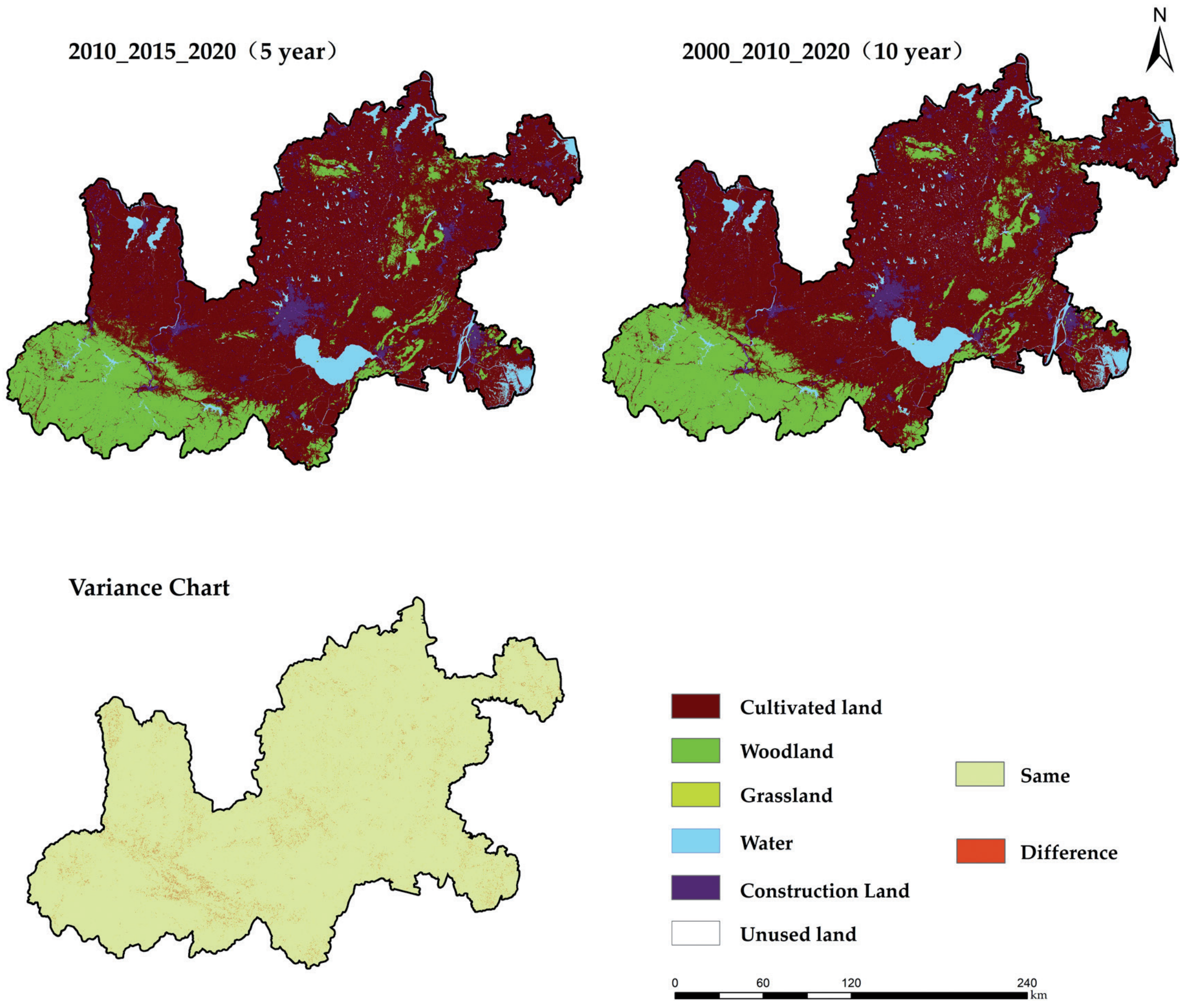

Fig. 6. Simulated differences at different time spans.

In the natural scenario, several notable changes in land use can be observed. Cultivated land decreases by 3,466.27 km^2, while forest land, water, and construction land increase by 1,996.56 km^2, 740.80 km^2, and 722.90 km^2 respectively. The changes in grassland and unused land are relatively insignificant. The main change is between cultivated land, forest land, and construction land, which accounts for the main differences in the landscape. In this scenario, construction land expands outward in areas characterized by higher levels of economic development. Within regions that encompass a mix of cultivated land and forest, the latter extends towards the periphery, resulting in a substantial reduction in the cultivated land area. The expansion of watersheds, observed mainly in the south-eastern region of the Yangtze River basin, stems from cultivated land. As a consequence, the natural scenario demonstrates a continuous expansion of construction land and forest land, along with a decrease in cultivated land. In contrast, the RD scenario shows the expansion of construction land as the dominant change, whereas other types of land experiencing varying degrees of reduction. Compared to the natural scenario, the RD scenario effectively curbs the reduction of cultivated land and stops the expansion of watersheds to meet development requirements. Moving to the CLP scenario, there is a significant expansion of cultivated land by 319.94 km^2, accompanied by a decrease in the growth of construction land. The expansion of cultivated land primarily occurs in areas where forest land is concentrated, with

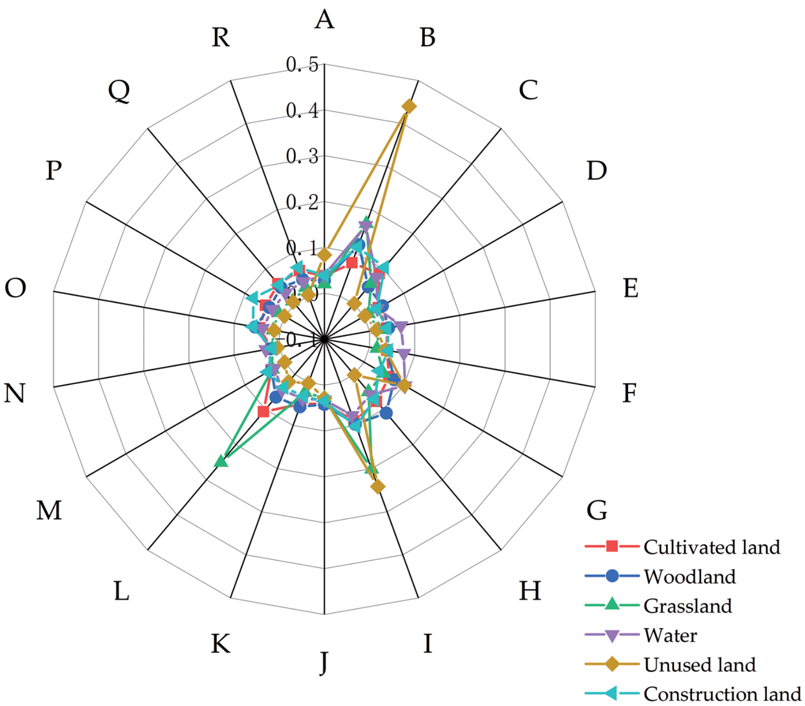

Fig. 7. Contribution of land use expansion drivers, 1990-2020. A: distance from city; B: DEM; C: distance from secondary road; D: distance from highway; E: GDP; F: distance from river; G: average annual rainfall; H: population; I: slope; J: distance from tertiary road; K: distance from school; L: average annual temperature; M: distance from railroad; N: soil attributes; O: distance to countryside; P: night light remote sensing; Q: distance to primary road; R: distance to town.

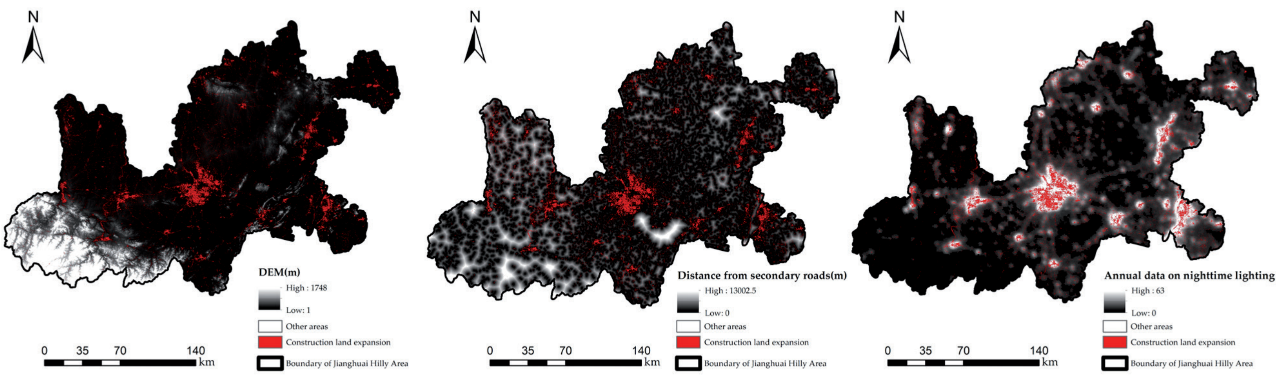

Fig. 8. Overlay of construction land expansion and factors.

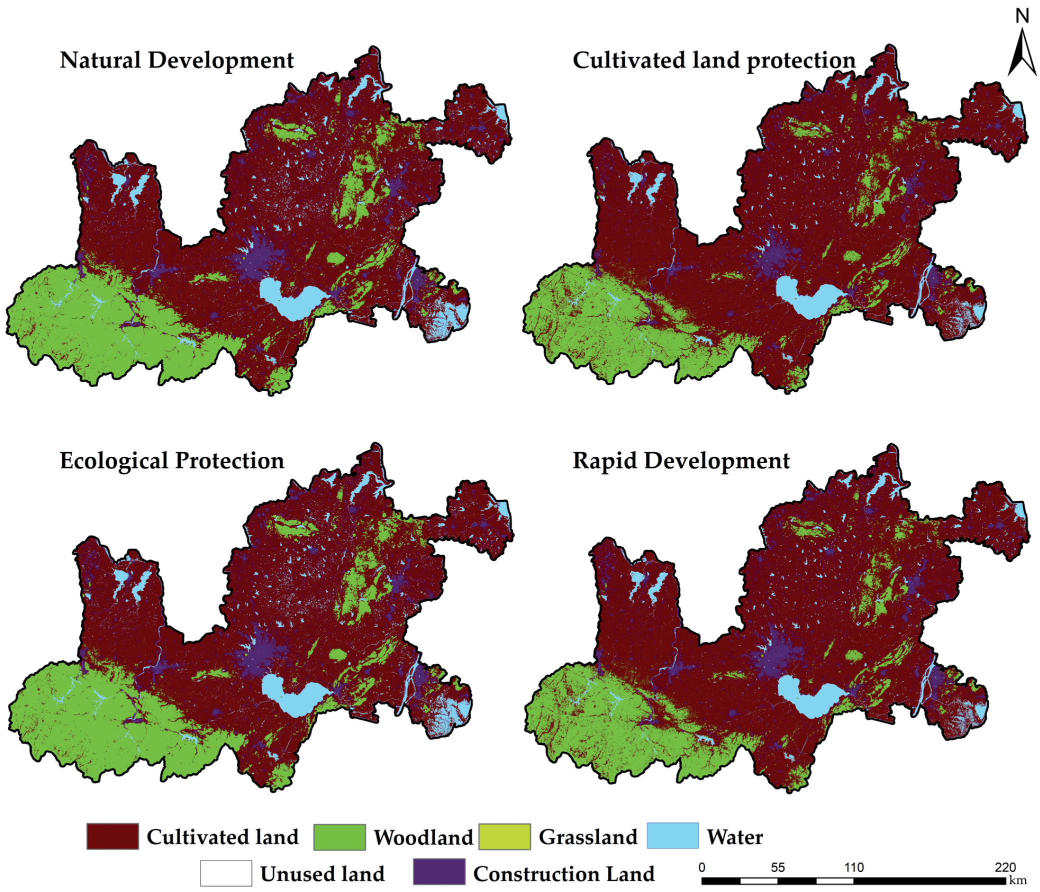

Fig. 9. Land use simulations for 2040 under different scenarios.

Table 7. Land use in 2040 under different scenarios.

	Scenario Model (2040)				Area status in 2020	Area change (km^2)			
	NP	RD	CLP	EP		NP	RD	CLP	EP
1	25642.56	28692.55	29428.77	27188.00	29108.83	-3466.27	-416.28	319.94	-1920.83
2	10311.45	8011.10	7994.15	9153.86	8314.89	1996.56	-303.79	-320.74	838.97
3	11.19	1.65	1.45	6.25	5.26	5.93	-3.61	-3.82	0.99
4	3609.05	2869.02	2869.04	3226.155	2868.25	740.8	0.77	0.79	357.91
5	0.37	0.30	0.21	0.35	0.61	-0.25	-0.32	-0.40	-0.26
6	4844.9	4844.9	4125.90	4844.9	4121.68	723.22	723.22	4.22	723.22

Note: NP-Natural Development; RD- Rapid Development; CLP- Cultivated land protection; EP- Ecological Protection; 1- Cultivated land; 2- Woodland; 3- Grassland; 4- Water; 5- Unused land; 6- Construction area.

the development of cultivated land being protected at the cost of ecological land and the constraints imposed by construction land. This scenario prioritizes food security but restricts economic development to some extent. Lastly, the EP scenario demonstrates a noteworthy decrease in cultivated land, while the total area of ecological land increases to 1197.87 km^2. This indicates a shift towards preserving and expanding ecological resources, necessitating a reduction in cultivated land.

An examination of the land use changes under the four different scenarios reveals distinct spatial allocations resulting from different development directions. The trends in nature protection NP and ecological development display similarities, with variations in the extent of expansion observed among different areas. Nonetheless, the overall direction of development remains consistent across the scenarios. In the RD scenario, economic development takes precedence, leading to a vigorous emphasis on urban construction while disregarding ecological security measures. Conversely, the CLP scenario prioritizes food security at the expense of ecological land security. Comparatively, the changes in other land types are less significant compared to the other three scenarios. A comprehensive assessment shows that the EP scenario holds greater promise for the development of JHHR. The land use combination in this scenario appears more rational, offering valuable insights for the optimal allocation of land resources and territorial spatial planning in JHHR's future.

Discussion

Land Use Change Factors

The current development strategy and direction of Anhui Province is "three zones, two highlands". Among them, JHHR, as the Yangtze River Economic Belt, needs to increase its support for the integrated development of the Yangtze River Delta, promote new urbanization and the development of urban agglomerations, create "inland open highlands" and "innovation-driven development highlands", and build an industrial system with the role of scientific and technological innovation and promoting opening up to the outside world [41]. The implementation of these development policies will have a series of effects on land use changes [42]. The development of modern industries and the promotion of urbanization will lead to an increase in demand for construction land, prompting the transformation of agricultural and ecological land into industrial and commercial land, causing the loss of cultivated land, environmental and EP and other issues [43, 44].

Before 2000, the change in the area of cultivated land was not obvious. The area of grassland decreased sharply during this period, while the expansion of built-up areas was the largest in 30 years. This findings is consistent with the results of Sai [45]. According to historical analysis, from 1990 to 2000, the JHHR focused on strengthening infrastructure construction, adjusting agricultural industrialization, transforming traditional agriculture into modern agriculture, and adjusting industrial layout at the same time [46]; from 2000 to 2010, the economic transformation and upgrading began, from traditional agricultural economy to ecological agriculture, characteristic agriculture and other diversified development directions, improving regional ecological quality, strengthening the protection and use of land resources [47]; from 2010 to 2020, with the "ecological+" development model, while the economic development focuses on green industries, ecological civilized cities, etc., the process of rural urbanization is accelerated, process of rural urbanization promote the construction of a new type of agricultural management system [48, 49].

Based on multi-scenario simulation, the land use model simulates future land use changes. By varying assumptions and parameter settings, different land use results can be simulated [50], which can help decision-makers assess the possible impact of policy implementation. The model can consider various factors such as population growth, economic development, and environmental protection, and explore the impact of interrelationships on land use, which makes up for the gaps in the research area.

Uncertainty and Outlook

Based on multi-period land use data, this paper comprehensively considers the driving factors such as natural and socio-economic factors, explores the inherent driving factors of land use change in the research area, combines various scenarios to simulate the future land use distribution structure, and provides decision-making suggestions for subsequent development. However, based on the complexity of the research content, there are still some shortcomings.

(1) The parameter settings in the PLUS model simulation are determined based on existing research results and continuous debugging. There is a certain subjectivity, and the uncertainty of the simulation results increases.

(2) Due to the limited and difficult access to data, the selection of driving factors cannot be considered comprehensively. Many factors such as biological species, geological movement, and social policies will have an impact on land use changes.

(3) The PLUS model is based on historical land use data and the probability of land expansion for simulation. It is difficult to reflect the real situation of land use changes due to changes in internal and external factors of real urban development.

Due to limitations such as the research area and research materials, there are certain deviations in the research results; In the analysis of the research results, only the influence between factors is considered, and there is a deviation from the actual situation. Subsequent optimization work can try to establish long-term monitoring samples and adjust them based on the actual local situation and related index parameters to improve the reliability and applicability of the model.

Conclusion

(1) The predominant land types in the JHHR are cultivated and woodland. In terms of spatial distribution, woodland is primarily located north of the southern boundary of the research area, whereas the remaining area is predominantly cultivated land. Over the past 30 years, land use changes have generally exhibited a stable trend. The most significant changes occurred between 2000 and 2005, with the highest dynamics observed in unused land and grassland. From 1990 to 2020, both cultivated land and woodland have experienced a decline, while the expansion of construction land has been continuous. The primary

types of land involved in these transformations are cultivated land and woodland.

(2) The land use simulation accuracy in the Jianghuai-Huai Hilly Region (JHHR) demonstrates superior performance. When considering various time spans for land use simulation predictions, the results consistently yield Kappa values exceeding 0.85 and overall accuracy surpassing 92%. These higher accuracy levels outperform other models, indicating the suitability of this model for future land use predictions.

(3) Utilizing the PLUS model for an in-depth analysis of land use expansion, we uncover the primary drivers behind the remarkable growth observed between 1990 and 2020. A comprehensive assessment reveals that factors like DEM, slope, and temperature significantly influence this expansion. Notably, cultivated land, woodland, grassland, water bodies, and unused land bear the imprint of both natural and human forces, shaping their trajectory. Conversely, the expansion of construction land predominantly reflects the interplay of socio-economic factors, underscoring their pivotal role in shaping the landscape.

(4) Examining the results of our multi-scenario simulation, it becomes apparent that the overall distribution of land use in the JHHR region will remain relatively stable by the year 2040. However, there are marked differences between the various scenarios, presenting noteworthy contrasts in land allocation. In the natural scenario, cultivated land experiences the most substantial decrease, while both woodland and construction land witness significant expansions. Conversely, the RD scenario places a primary emphasis on the expansion of construction land, resulting in varying degrees of decline for other land types. Under the CLP scenario, the growth of cultivated land demonstrates an upward trend, although its progression is overshadowed by other scenarios, and limitations on construction land expansion persist. Notably, in the EP scenario, there is a concerted effort to safeguard ecological land, accompanied by discernible increases in other land categories.

Taking a comprehensive view and considering a range of factors, the EP scenario emerges as the optimal model for future development in the research area. This scenario provides decision-makers with valuable insights when formulating strategies for efficient spatial arrangement.

Acknowledgments

We sincerely thank Wuhan University Remote Sensing Information Processing Research and the Chinese Academy of Sciences for their data support and help to all of us. We express our sincere gratitude to our friends and partners for their kind advice and moral support.

Conflict of Interest

The authors declare no conflict of interest

References

1. QIU L., ZHU J., WANG K., HU W. Land Use Changes Induced County-Scale Carbon Consequences in Southeast China 1979-2020, Evidence from Fuyang, Zhejiang Province. Sustainability. **8** (1), 38, **2015**.
2. XI C., YING Q.F., JUN Z.H., DAN D., YING X.Y., KHUKHUUDEI U. Effects of climate variability and land use/land cover change on the Daihai wetland of central Inner Mongolia over the past decades. Journal of Mountain Science. **17** (12), 3070, **2020**.
3. ZHIBO L., QIAN S., JIANYUN Z., SHIRU W. Prediction and Evaluation of Ecosystem Service Value Based on Land Use of the Yellow River Source Area. Sustainability. **15** (1), 687, **2022**.
4. YE, JING, HOU, ZHIJIE, MING, HAIYAN, CHENG, YEHUAI Ecological security pattern-based simulation for land use structure change: a case study in Ezhou City, China. Frontiers of Earth Science. **15** (3), 1, **2021**.
5. DEHE X., KE Z., LIANHAI C., XIANGRONG G., HENGBIN Z. Driving forces and prediction of urban land use change based on the geodetector and CA-Markov model: a case study of Zhengzhou, China. International Journal of Digital Earth. **15** (1), 2246, **2022**.
6. LIHAN C., WENWEN T., SHENG Z., P. S. R. Ecological Protection Alone Is Not Enough to Conserve Ecosystem Carbon Storage: Evidence from Guangdong, China. Land. **12** (1), 111, **2022**.
7. SHUYING J., JUNRAN L., YONGQIANG L., ZIYUN X., BAISHU K., YE L., YUWEN S. Variation of soil organic carbon and physical properties in relation to land uses in the Yellow River Delta, China. Scientific Reports. **10** (1), 20317, **2020**.
8. LONGHUI L., AN H., YUEQING X., RAYMUNDO M., YAMING D., ZHENGXIN J. The Influences of Livelihood and Land Use on the Variation of Forest Transition in a Typical Mountainous Area of China. Sustainability. **12** (22), 9359, **2020**.
9. XUFENG C., CUICUI L., LING S., JIAQI L., JING Z., YUEHUA J., GUANGHONG Z. Spatial-Temporal Responses of Ecosystem Services to Land Use Transformation Driven by Rapid Urbanization: A Case Study of Hubei Province, China. International Journal of Environmental Research and Public Health. **19** (1), 178, **2021**.
10. LINA G., FEI T., RUNRUI L., ZILONG W., HONGJUN L., TONG Z. Multi-scenario simulation and ecological risk analysis of land use based on the PLUS model: A case study of Nanjing. Sustainable Cities and Society. **85**, **2022**.
11. ZHOU L., DANG X., SUN Q., WANG S. Multi-scenario simulation of urban land change in Shanghai by random forest and CA-Markov model. Sustainable Cities and Society. **55** (C), 102045, **2020**.
12. ZHANG F., LIU X., ZHANG J., WU R., MA Q., CHEN Y. Ecological vulnerability assessment based on multi-sources data and SD model in Yinma River Basin, China. Ecological Modelling. **349**, 41, **2017**.
13. CHUYU X., JIAN Z., JING Z., FEI X., QIANG L., KAI F., ZHUANG S., JIAN Z., SONG L., JUN Z. Exploring potential of urban land-use management on carbon

emissions – A case of Hangzhou, China. Ecological Indicators. **146**, **2023**.
14. ZHENJIE L., LIJUAN Z. Spatio-temporal analysis and simulation of urban ecological resilience in Guangzhou City based on the FLUS model. Scientific Reports. **13** (1), 7400, **2023**.
15. WANG Y., SHEN J., YAN W., CHEN C. Backcasting approach with multi-scenario simulation for assessing effects of land use policy using GeoSOS-FLUS software. MethodsX. **6** (C), 1384, **2019**.
16. YAO L., JIULIN L., JINLONG C. Research on land-use evolution and ecosystem services value response in mountainous counties based on the SD-PLUS model. Ecology and Evolution. **12** (10), 9431, **2022**.
17. JUAN W., JIAQI L., WENPING Z., TIANQIAN C., YANG Y., JINJIN W. Land-Use Pattern Evaluation Using GeoSOS-FLUS in National Territory Spatial Planning: A Case Study of Changzhi City, Shanxi Province. Sustainability. **14** (21), 13752, **2022**.
18. XUN L., QINGFENG G., C. C. K., SHISHI L., BINGYU W., YAO Y. Understanding the drivers of sustainable land expansion using a patch-generating land use simulation (PLUS) model: A case study in Wuhan, China. Computers, Environment and Urban Systems. **85**, 101569, **2021**.
19. LIHUA C., YUAN M. Current and future characteristics of land use based on intensity analysis and PLUS model : a case study of Foshan city, China. SN Applied Sciences. **5** (3), **2023**.
20. SHIHE Z., QUANLIN Z., DONGLIANG C., CHAOBIN X., YUNNI C., YUYING L., BAOYIN L. Landscape ecological risk projection based on the PLUS model under the localized shared socioeconomic pathways in the Fujian Delta region. Ecological Indicators. **136**, **2022**.
21. NIU TONGLI X.L., CHEN JIE, ZHOU YANLAI, YIN JIABO, LIU DEDI. Land use simulation and multi-scenario prediction of the Yangtze River Basin based on PLUS model. Engineering Journal of Wuhan University. 1, **2023**.
22. LI JUN Y.D., WU FENGZHEN, CHEN RUJUN, HE WANCAI Dynamic Simulation of Land Use Changes and Assessment of Carbon Storage in Kunming City Based on PLUS and In VEST Models. Bulletin of Soil and Water Conservation. **43** (01), 378, **2020**.
23. XINGYUAN X., XIAO H., LINLONG J., CAIXING J. Empirical study on comparative analysis of dynamic degree differences of land use based on the optimization model. Geocarto International. **37** (25), 9847, **2022**.
24. ZHANG R., PU L., ZHU M. Impacts of transportation arteries on land use patterns in urban-rural fringe: A comparative gradient analysis of Qixia District, Nanjing City, China. Chinese Geographical Science. **23** (3), 378, **2013**.
25. PRASAD V.K., KANT Y., BADARINATH K.V.S. Land use changes and modeling carbon fluxes from satellite data. Advances in Space Research. **30** (11), 2511, **2002**.
26. SHI G., JIANG N., YAO L. Land Use and Cover Change during the Rapid Economic Growth Period from 1990 to 2010: A Case Study of Shanghai. Sustainability. **10** (2), 426, **2018**.
27. FENG L., XINGWEI C., HUAXIA Y., FENGYI L. SWAT model-based quantification of the impact of land-use change on forest-regulated water flow. Catena. **211**, **2022**.
28. XIAOYANG L., MING W., ZHIGANG L., JIAN Z. Multi-scenario simulation of urban growth boundaries with an ESP-FLUS model: A case study of the Min Delta region, China. Ecological Indicators. **135**, **2022**.
29. XIAOQIONG L., XU W., KUNLUN C., DAN L. Simulation and prediction of multi-scenario evolution of ecological space based on FLUS model: A case study of the Yangtze River Economic Belt, China. Journal of Geographical Sciences. **33** (2), 373, **2023**.
30. JUN L., JIYAN W., JUNNAN X., WEIMING C., XINGJIE C., WEN H., YUFENG H., YU D., GANG Y., NAN W. Dynamic Assessment of the Flood Risk at Basin Scale under Simulation of Land-Use Scenarios and Spatialization Technology of Factor. Water. **13** (22), 3239,**2021**.
31. GUOQIANG M., QIUJIE L., JINXIU Z., LIXUN Z., HUA C., ZHENGPING J., GUOJUN S. Simulation and Analysis of Land-Use Change Based on the PLUS Model in the Fuxian Lake Basin (Yunnan-Guizhou Plateau, China). Land. **12** (1), 120, **2022**.
32. XIAOFU L., HUI F. Spatial-Temporal Evolution and Driving Forces of Cultivated Land Based on the PLUS Model: A Case Study of Haikou City, 1980-2020. Sustainability. **14** (21), 14284, **2022**.
33. HAO L., HONGYU C., MINGHAO W., KAI Z., XIANG Z., ZHICHENG L. A Dynamic Evaluation Method of Urban Ecological Networks Combining Graphab and the FLUS Model. Land. **11** (12), 2297,**2022**.
34. XIN C., XINYI H., SIYUAN W. Simulated Validation and Prediction of Land Use under Multiple Scenarios in Daxing District, Beijing, China, Based on GeoSOS-FLUS Model. Sustainability. **14** (18), 11428, **2022**.
35. PENG H., JINGWEI X., QINGLIN Z. Spatial differentiation and scenario simulation of cultivated land in mountainous areas of Western Hubei, China: a PLUS model. Environmental science and pollution research international. **30** (18), 52804, **2023**.
36. JINBING Z., HUIRU Z., PENGYAN Z., YONGPENG S., YING Z., YANYAN L., TIANQI R., ZHENYUE L., DAN Y., YUANYUAN L. Construction of GI Network Based on MSPA and PLUS Model in the Main Urban Area of Zhengzhou: A Case Study. Frontiers in Environmental Science. **2022**.
37. YI Z., MINRUI Z., BO Q. Optimization of spatial layout based on ESV-FLUS model from the perspective of "Production-Living-Ecological": A case study of Wuhan City. Ecological Modelling. **481**, **2023**.
38. LIANG X., LIU X., LI X., CHEN Y., TIAN H., YAO Y. Delineating multi-scenario urban growth boundaries with a CA-based FLUS model and morphological method. Landscape and Urban Planning. **177**, 47, **2018**.
39. ZHIQIANG L., SHUANGYUN P. Comparison of multimodel simulations of land use and land cover change considering integrated constraints - A case study of the Fuxian Lake basin. Ecological Indicators. **142**, **2022**.
40. LIU Y., SHI J., ZHENG Y., HUANG X. The Evolution Pattern and Simulation of Land Use in the Beijing Municipal Administrative Center (Tongzhou District). Journal of Resources and Ecology. **13** (2), 270, **2022**.
41. LIANG P., BIN D., PING W., SHUWEI S., LI S., LEI F., HAORAN L., LIPING L. Research on ecological risk assessment in land use model of Shengjin Lake in Anhui province, China. Environmental geochemistry and health. **41** (6), 2665, **2019**.
42. JINQUAN Z., YASHA W., YAJUN G. Evaluating the Relationship between Urban Population Growth and Land Expansion from a Policymaking Perspective: Ningbo, China. Journal of Urban Planning and Development. **146** (4), **2020**.

43. COLSAET A., LAURANS Y., LEVREL H. What drives land take and urban land expansion? A systematic review. Land Use Policy. **79**, 339, **2018**.
44. WANG K., LI Z., ZHANG J., WU X., JIA M., WU L. Built-up land expansion and its impacts on optimizing green infrastructure networks in a resource-dependent city. Sustainable Cities and Society. **55** (C), 102026, **2020**.
45. HU S., CHEN L., LI L., ZHANG T., YUAN L., CHENG L., WANG J., WEN M. Simulation of Land Use Change and Ecosystem Service Value Dynamics under Ecological Constraints in Anhui Province, China. International Journal of Environmental Research and Public Health. **17** (12), 4228, **2020**.
46. YONG L.X.R.Q.L. Evaluation of regional land use performance based on entropy TOPSIS model and diagnosis of its obstacle factors. Editorial Office of Transactions of the Chinese Society of Agricultural Engineering. **32** (13), 243, **2016**.
47. JINLING Z., JIE W., YU J., LINGLING F., CHAO X., DONG L., LINSHENG H. Land Cover Based Landscape Pattern Dynamics of Anhui Province Using GlobCover and MCD12Q1 Global Land Cover Products. Sustainability. **10** (4), 1285, **2018**.
48. YUTING Y., GUANGHUI J., QIUYUE Z., DINGYANG Z., YULING L. Does the land use structure change conform to the evolution law of industrial structure? An empirical study of Anhui Province, China. Land Use Policy. **81**, 657, **2019**.
49. SAI H., LONGQIAN C., LONG L., BINGYI W., LINA Y., LIANG C., ZIQI Y., TING Z. Spatiotemporal Dynamics of Ecosystem Service Value Determined by Land-Use Changes in the Urbanization of Anhui Province, China. International journal of environmental research and public health. **16** (24), 5104, **2019**.
50. XIUFENG C., ZHAOSHUN L., SHUJIE L., ZHENJUN G. Integrating the Ecological Security Pattern and the PLUS Model to Assess the Effects of Regional Ecological Restoration: A Case Study of Hefei City, Anhui Province. International Journal of Environmental Research and Public Health. **19** (11), 6640, **2022**.